FACULDADE DE ENGENHARIA DA UNIVERSIDADE DO PORTO

# Optimal Control of Power Kites for Wind Power Production

**Tiago Costa Moreira Maia**

Master in Electrical and Computers Engineering

Supervisor: Fernando Arménio da Costa Castro e Fontes

Co-Supervisor: Luís Tiago de Freixo Ramos Paiva

October 15, 2014

U.PORTO
FEUP FACULDADE DE ENGENHARIA
UNIVERSIDADE DO PORTO

**MIEEC - MESTRADO INTEGRADO EM ENGENHARIA ELETROTÉCNICA E DE COMPUTADORES** | **2013/2014**

A Dissertação intitulada

"Optimal Control of Power Kites for Wind Power Production"

foi aprovada em provas realizadas em 08-10-2014

**o júri**

Presidente Professor Doutor Fernando Manuel Ferreira Lobo Pereira
Professor Catedrático do Departamento de Engenharia Eletrotécnica e de Computadores da Faculdade de Engenharia da Universidade do Porto

Professor Doutor José Manuel do Valle Cardoso Igreja
Professor Coordenador do Departamento de Engenharia Eletrotécnica - Energia e Automação da Instituto Superior de Engenharia de Lisboa

Professor Doutor Fernando Arménio da Costa Castro e Fontes
Professor Associado do Departamento de Engenharia Eletrotécnica e de Computadores Faculdade de Engenharia da Universidade do Porto

O autor declara que a presente dissertação (ou relatório de projeto) é da sua exclusiva autoria e foi escrita sem qualquer apoio externo não explicitamente autorizado. Os resultados, ideias, parágrafos, ou outros extratos tomados de ou inspirados em trabalhos de outros autores, e demais referências bibliográficas usadas, são corretamente citados.

Tiago Maia

Autor - Tiago Costa Moreira Maia

Faculdade de Engenharia da Universidade do Porto

# Resumo


As turbinas eólicas atuais já atingiram o pico da sua capacidade. A instabilidade do vento, o custo elevado das instalações e a baixa potência gerada são algumas das limitações do design atual. A indústria da energia eólica, de modo a tornar-se mais competitiva, tem de encontrar novos métodos para extrair energia do vento.

A superfície terrestre cria o efeito da camada limite, que influencia o vento, fazendo aumentar a sua velocidade com a altitude. De facto, com a altitude, o vento não só é mais forte como também é mais estável. De modo a capitalizar estas fortes correntes, novas formas de extração de energia eólica estão a ser propostas. Uma destas soluções baseia-se num papagaio que ativa um gerador através das linhas que o ligam à terra. Este novo conceito permite uma potência muito maior por unidade.

Neste documento, é apresentado o modelo do papagaio. Em seguida é feita uma simulação do modelo usando o método de Euler. Posteriormente é implementado, recorrendo ao software de controlo ótimo ACADO toolkit, o problema de controlo ótimo de modo a se obter uma trajetória em forma de "oito" maximizando a potência gerada. Finalmente é também implementado em ACADO um MPC de modo a se solucionar o problema de controlo ótimo, desta vez inserindo várias perturbações.

# Abstract

Ground based wind energy systems have reached the peak of their capacity. Wind instability, high cost of installations and small power output of a single unit are some of the the limitations of the current design. In order to become competitive, the wind energy industry needs new methods to extract energy from the wind.

The Earth's surface creates a boundary layer effect on the wind that increases its speed with altitude. In fact, with altitude the wind is not only stronger, but steadier. In order to capitalize these strong streams new extraction methods were proposed. One of these solutions is to drive a generator using a tethered kite. This concept allows very large power outputs per unit.

In this document, firstly, the kite model is presented. Afterwards, a simulation is run using the euler method. To find an optimal solution with a form of "eight" trajectory, the control problem is implemented using an optimal control software - ACADO toolkit in order to maximize the power output. Finally, using a MPC strategy, the optimal control problem is solved again, but this time with wind perturbations.

# Agradecimentos

Em primeiro lugar queria deixar um enorme obrigado aos meus orientadores, Professor Fernando Fontes e Luís Tiago Paiva, pelo apoio fulcral que foram dando durante a realização desta dissertação. Sempre disponíveis para tirar qualquer dúvida que surgisse. Foram, sem dúvida, essenciais para a realização com sucesso deste trabalho.

À minha família, pricipalmente à Lina, ao Neca e ao André, por me apoiarem todos os dias e me darem a oportunidade, não só de estudar, mas também de aproveitar todas as oportunidades que foram surgindo ao longo da minha vida, mesmo que isso às vezes implicasse uma noite mal dormida.

Aos meus amigos, por todos os momentos partilhados ao longo da vida. A sua companhia, conselhos e influência definiram muito da pessoa que sou hoje.

Aos ervilhinhas, se não fossem vocês não teria metade das histórias para contar à lareira, no Natal, aos meus netos.

To all my friends I met during my Erasmus in Ghent. If it was not you I would not be finishing my master degree now. I would have finished it one year ago, but I would not have one of the best (if not the best) year of my life.

A JBARdinagem por todas as noites da Queima das Fitas (in)esquecíveis.

Por fim, gostaria de deixar uma palavra especial aos meus colegas que me acompanharam num projeto muito especial para mim que é a Tuna de Engenharia da Universidade do Porto.

Tiago Maia

*"All the world is made of faith, and trust, and pixie dust."*

Peter Pan

# Contents

# List of Figures

# List of Tables

# Acronyms

| | |
|---|---|
| ACADO | An Open Source Framework for Automatic Control and Dynamic Optimization |
| BFD | Backward Differentiation Formula |
| DAE | Differential Algebraic Equation |
| HWE | High Wind Energy |
| KKT | Karush–Kuhn–Tucker |
| MATLAB | Software for numerical computation, visualization and programming |
| MPC | Model Predictive Control |
| OC | Optimal Control |
| OCP | Optimal Control Problem |
| ODE | Ordinary Differential Equation |
| SQP | Sequential quadratic programming |
| WT | Wind Turbine |
| WTG | Wind Turbine Generator |

# Chapter 1

# Introduction

## 1.1 Context

In wind resides a potential solution to the current power demand. Despite having been used for centuries to grind grain, pump water, propel sailing ships across oceans, among others, wind has not yet reached its full potential [11]. The current technology based on wind mills is far from being a competitive alternative against the fossil sources. Indeed, the current renewable sources will not contribute with more than 20% within the next 15 to 20 years. Even though wind mills are the largest supplier of renewable energy (excluding hydro power plants), when compared, the generated power density per $km^2$ of a wind mill, it is 200 to 300 times lower than that of a thermal plant [12]. This is due to a number of contributing factors. For instance, a wind turbine generator (WTG) requires heavy foundations and huge blades which represents a massive investment and leads to a significant ground occupation. Another factor is the variability of wind speed at low altitudes.

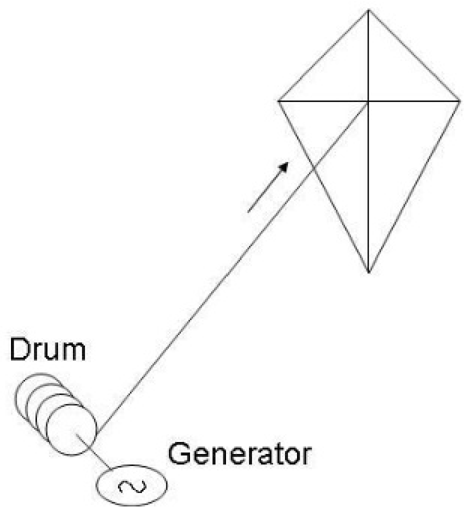


Figure 1.1: Simple illustration of a power kite [1].

Actually, the current ground based wind energy systems have, basically, reached the peak of their capacity [1]. In order to overcome such limitations the development of technology that could take advantage of the fact that wind speed generally increases with altitude, where stronger and steadier streams are available, began [8, 1]. The basic idea is to collect the potential energy of these streams with a tethered airfoil, like a power kite (Figure 1.1). The energy transferred by the kite lines would be transformed at ground level by converting the mechanical power into electric power.

## 1.2 Motivation

In the current scenario, kites have become one of the most promising applications to generate electric power. The kite is connected to the ground to a drum capable of paying the cable in and out. Power is generated during the reel-out phase, which is when the line is at higher tension, and spent during the reel-in when the line is at lower tension. The tension can be controlled by pulling the kite lines. By doing this, it will be possible to control the forces on the kite and subsequently, the kite angle of attack. As the kite angle is increased, the tension also increases and the kite is lifted, generating power. The opposite happens when the angle is decreased. The biggest the gap in the tension during both phases, the biggest the power output of the system [13]. It is this ability to be manoeuvred that is most appealing [14].

The aim of this dissertation is to study and design a possible control method for one of these kites in order to enhance its power production.

It is expected that a wind power generator of this kind will have a power production capacity per unit 5000 to 10000 times larger than a conventional WTG. The installation and rent costs per unit will be lower and no noise pollution will be emitted [11].

## 1.3 Objectives

This thesis studies the optimal means of flying a kite to maximize its power output.

To reach this goal the following objectives are considered:

- **R**eview technologies and principles of high wind power extraction.
- **S**tudy of the kite and wind model.
- **C**ontrol Problem using a path following strategy and possible solutions.
- **S**ensitivity analysis of the proposed solution.

## 1.4 Document Structure

This document is organized as follows. In Chapter 2 the state of art and all the related work in this field are presented. Chapter 3 introduces the kite and wind model. The control problem and possible solutions are studied in Chapter 4. In Chapter 5 some conclusions of this work are drawn.

# Chapter 2

# State of the Art

This Chapter studies the wind conditions at high altitude. Afterwards, some solutions and methods to extract power from the high wind are discussed. In the following section the method that will be studied in this document is introduced as well as the currently used power kite actuators.

## 2.1 High Wind Energy

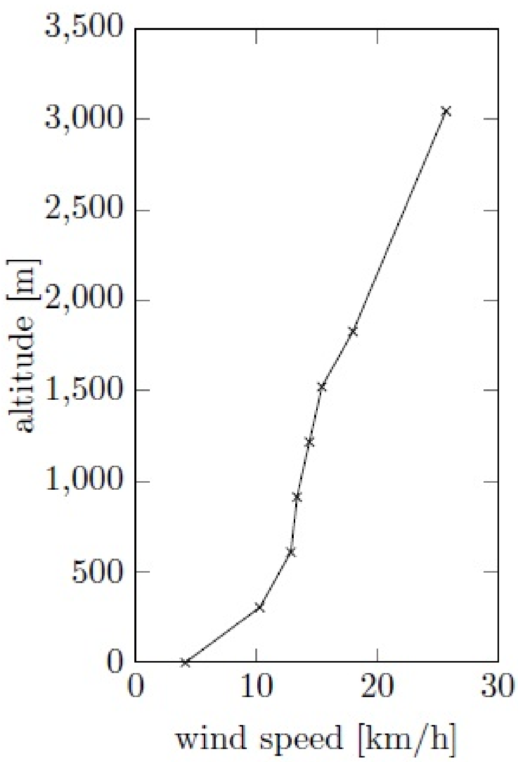


(a) Average wind velocity profile. Brussels 30-05-2012.

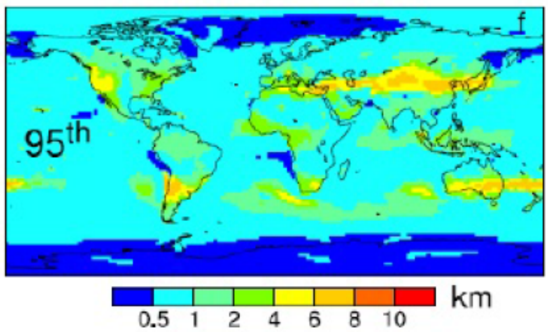


(b) Altitude of wind power density(95$^{th}$ percentile of annual average).

Figure 2.1: Airborne wind energy systems can profit from higher wind speeds at altitude [2].

The power extracted from a WTG strongly depends on the wind speed. Unfortunately, the wind is relatively slow close to the ground and, sometimes, is non-existent what makes the power production less efficient.

The Earth's surface creates a boundary layer effect so that wind speed increases generally with altitude. Although the true wind patterns depend on a variety of factors like the Earth's rotation, the solar flux, among others, the wind in the troposphere and stratosphere is mostly present even when there is no wind at ground level. With steadier and more predictable winds, high-altitude wind has an advantage over wind near the ground.

As it can be seen in Figure 2.1 there are two major jet streams: the Polar Front Jet and the Sub-Tropical Jet, both located between 30 and 40 degrees in each hemisphere. The wind speed in the jet streams is permanent and can reach 40 m/s and in some parts even more. This is a very significant wind source, since the near the surface wind is on the order of the 5 m/s. Moreover, the power generated by the WTG's not only increase with the wind speed, but rather by the cube of it [13, 11].

## 2.2 High Wind Energy Systems

The idea of using high wind energy (HWE) goes as back as the 1930s. In the late 1960s, a company named Sheldahl, Inc. placed a generator on a tethered balloon and generated about 350 Watts of power [15]. In the mid 70s several proposals placed to the National Science Foundation and the Energy Resources Development Administration in the United States, were denied because of the possible hazards to aircraft and were classified as non profitable. This has not stopped further research, and advances in technology caused this idea to persist in a way that proposals for such systems are still being made [1]. In this section, such proposals will be presented.

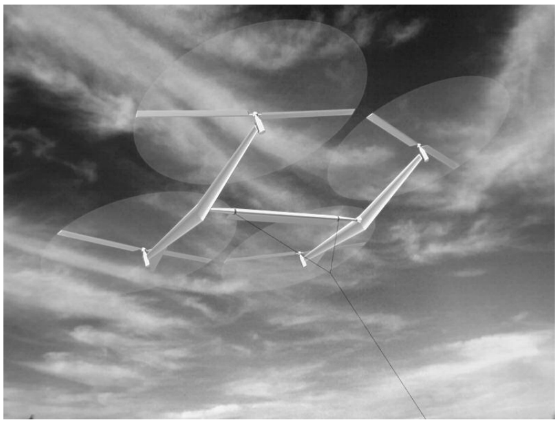

Figure 2.2: Quadruple rotor arrangement [3].

In 1983, Riedler and Riegler proposed using a WTG mounted on a tethered balloon. Six symmetrically arranged turbines were attached to the balloon just behind its center of gravity [16]. A system consisting of a platform with rotary wings to provide power from the jet stream was

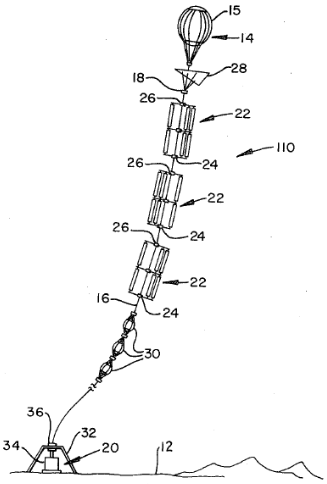

(a) Wind driven high altitude power apparatus [18].

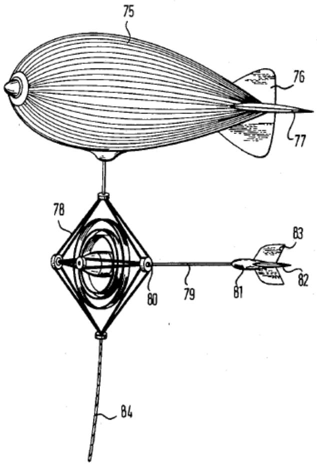

(b) Wind driven power plant [19].

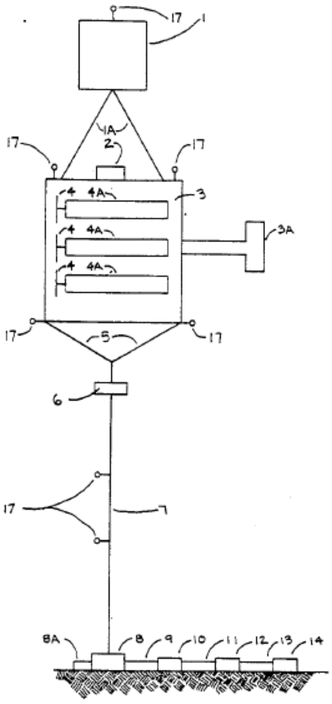

(c) Wind generator kite system [20].

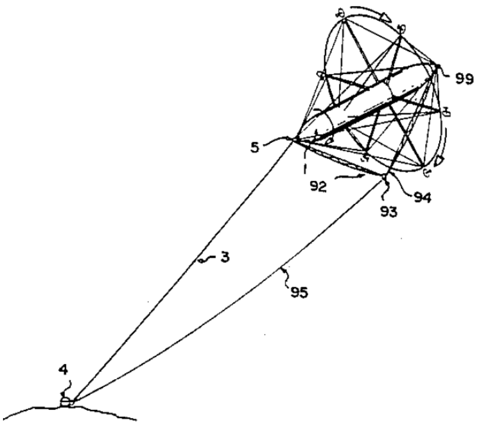

(d) Airship-floated wind turbine [21].

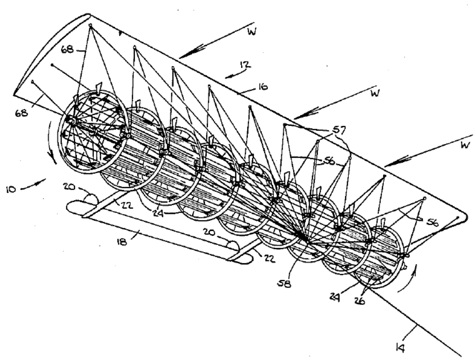

(e) Drum kitecraft [22].

Figure 2.3: Examples of high wind systems with lifted generators.

also studied. The power would be transmitted to the ground by means of a tethered cable with aluminium conductors [17]. Recently, this concept was studied and improved. The main design uses an airframe with two or more rotors inclined at a controlled angle to the wind stream (Figure 2.2). The rotors not only are used to produce electricity but also to keep the frame up in the air. The power is transmitted to the ground via an aluminium-Spectra composite (Spectra is a high strength fibre). The frame would have to land from time to time depending on the wind speed [3].

In 1978, Fri and Hise suggested a tethered balloon with wind driven rotors fixed along the length of a flexible power shaft. The lower end of the shaft is connected to a ground supported energy conversion device (Figure 2.3a) [18].

Another system consisted in a tethered aerostat carrying at least one rotor and a current generator coupled to it (Figure 2.3b) [19].

In 1984, Pugh proposed a wind power generator suspended in the air like a kite and connected to the ground by high strength cables. The small wind generators would be mounted in the kite and raised to the desired altitude by a gas balloon (Figure 2.3c) [20].

One year later, a system using an airship floated wind turbine was proposed. It was connected to the ground by two tethers, through which the power was conducted (Figure 2.3d) [21].

Later, 1987, an invention named kitecraft was secured to a ground tether supporting a cylindrical drum. The drum consists in many wheels interconnected by airfoils. Wind action on the airfoils rotates the drum turning the generator to provide electric power (Figure 2.3e) [22].

All these systems had the drawback of having the power generator up in the air. This increased significantly the weight of the system and consequently the difficulty of launching, lifting and keep it flying. An alternative was first introduced in 2001, where generator was placed on the ground and the cable was moved through the generator by a high lifting body, like a kite or a balloon(Figure 2.4). The wings on the upside operate at high angle of attack in order to generate high lift to pull the cable upwards. On the downside, the wings have an angle of attack as small as possible to reduce the drag. The difference in tension causes the cable to be pulled through the generator, generating power. The wings would be made of a light material so in case of a fall, no harm will come to the people or buildings around [4].

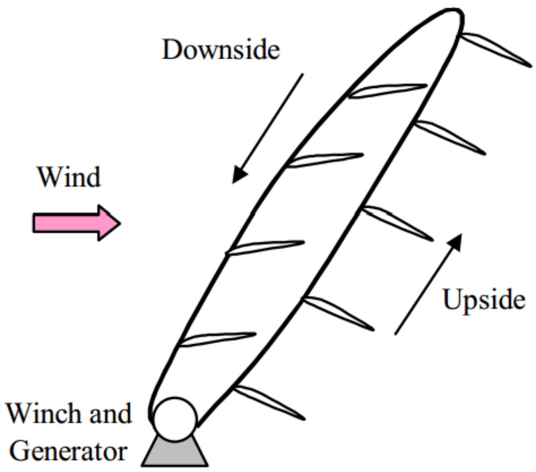


Figure 2.4: The original laddermill concept [4].

An alternative concept of the laddermill consists in a single cable being pulled through a generator. Instead of being pulled continuously around the generator, it would be pulled up and down it. This is, indeed, a much lighter-weight option and a lot simpler [23].

It is clear that the systems differ in one main aspect: the location of the generator. Newer proposals place it on the ground instead of up in the atmosphere. In the next section the laddermill model will be studied in more detail.

## 2.3 The Laddermill

The laddermill concept uses lifting bodies, like kites, flying into the higher regions of the atmosphere. In order to have a better perspective of the problem a simpler model of the laddermill will be considered. This model consists of only one lifting body as in Figure 1.1. The actual laddermill will have several kites connected to the cable. The lower part of the cable, about 10 %, is wound around a drum. The tension created by the kite pulls the generator up to produce power. To maximize the output, the kite trajectory must be controlled. This can be achieved by lowering the attack angle during the descent and the opposite during the ascending. One possible ideal trajectory resembles a the figure of number eight as can be seen in Figure 2.5.

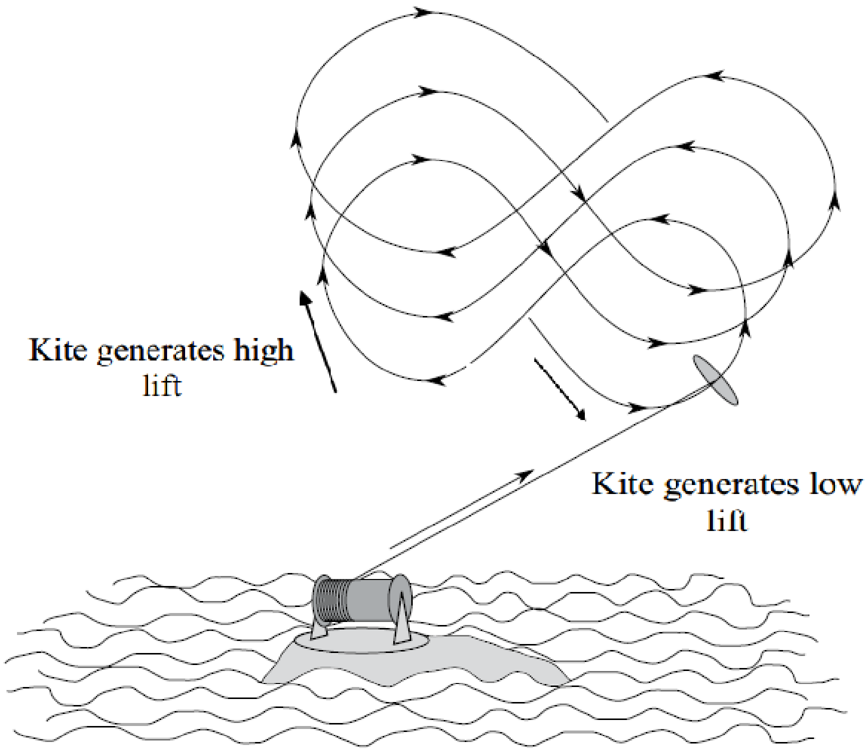


Figure 2.5: A kite generator and a possible ideal trajectory [5].

The higher the difference between the tension during the descend and the ascend, the higher the power output and consequently, the efficiency. In order to study a possible optimal trajectory, the kite model must be studied. A possible model is presented in the following section.

## 2.4 Kite Control Actuators

Remote control of power kites is achieved through the use of some mechanisms. Despite several kites optimized for laddermill use, the kites currently used in research are mostly derive from commercial available surfing kites. A surfing kite is usually controlled using a handle bar. Steering lines are attached to both sides of the bar, leading up to the tips of the kite. This enables the surf to control both the angle of attack and to steer the kite in a certain direction. The same principles are applied to the remote controlled kite.

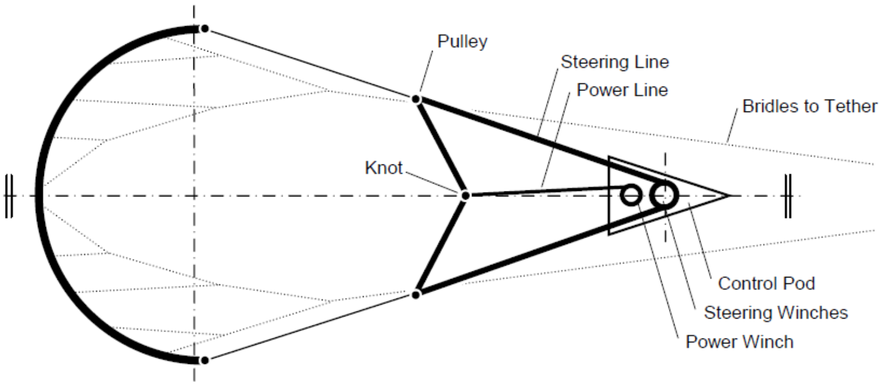


Figure 2.6: Kite with airborne steering mechanism [6].

The control pod of a typical system in represented in Figure 2.6. It contains two motors, one for steering the kite and one for controlling the power setting. In this system, there are two winches on the steering motor, each wind up one end of the steering line, so that when one end is released, the other is pulled. As an asymmetric wingtip load is applied, the kite begins to turn. Only one winch is connected to the power motor. Winding up the power line applies a symmetrical load to the wingtips, which leads to an increase in the angle of attack [6].

Figure 2.7: Wingtip AoA control [1].

Another possible way of controlling the angle of attack is by installing a winch servo (Figure 2.7). This cause additional drag on that side together with a side force, causing the kite to yaw.

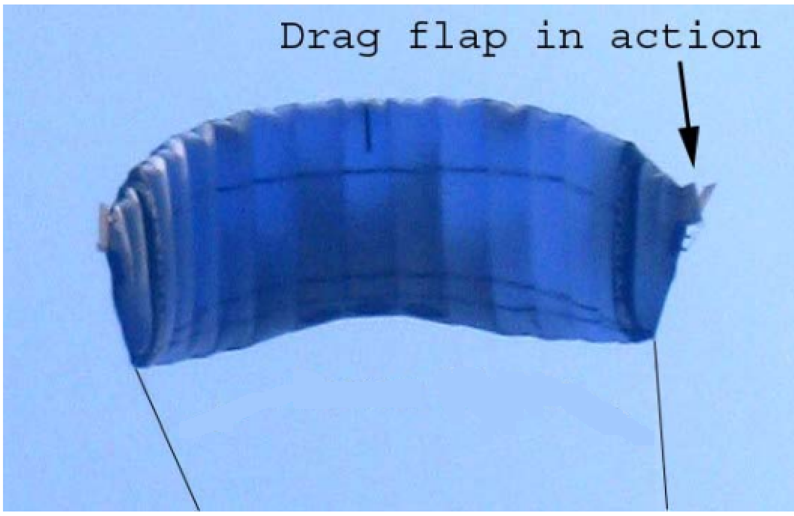


Figure 2.8: Drag flap control mechanism [7].

The control system in Figure 2.7 uses a small servo to activate drag flaps on the side of the kite. This control mechanism only works on a stable kite because the force generated is quite small. The drag force creates a deviation from the equilibrium, causing the kite to yaw.

The latest control mechanism steers the kite by changing the attachment point of the steering line on the kite. The slide mechanism has been demonstrated to work very well on many different types of surf kites (Figure 2.9) [1].

Figure 2.9: Slide mechanism on the kite [1].

An important question is the location of the control pod. Implementing the actuators as part of the ground station eliminates additional drag and weight, which have positive effects on the aerodynamic properties of the kite (Figure 2.10a).

On the other hand, an airborne control pod (Figure 2.10b) has minimal mechanical delay between activation of the winches and the dynamic response of the wing. Another advantage is the ability to be controlled if the main tether ruptures. It is also easier to reel in and out a single main tether than both steering lines, while still enabling full control over the kite [6, 24].

(a) Ground control pod [25].

(b) Airborne control pod [24].

Figure 2.10: Different types of control pods.

## 2.5 Discussion

In this chapter, the research work that so far has been done in the field of power extraction from high wind was presented . Many systems were presented that could be used to make this power source profitable. As it could be seen, the main difference between different systems resides in the place where is the generator placed, on the ground or up in the atmosphere. Placing the generator in the ground reduces the weight of the system making it easier to lift and safer is case of a crash.

Even though the laddermill is still an emerging topic, already some research has been done in this field. This system has the advantage of having a ground generator and the materials used to build the kites are light, which makes it safer without compromising its efficiency.

The simplified kite model presented will be used to study an optimal trajectory of the kite in order to maximize the power output.

# Chapter 3

# Kite Model

This chapter describes the kite model of the tethered kite system that was used in this document and is derived from one firstly used in [26].

## 3.1 Mathematical Model

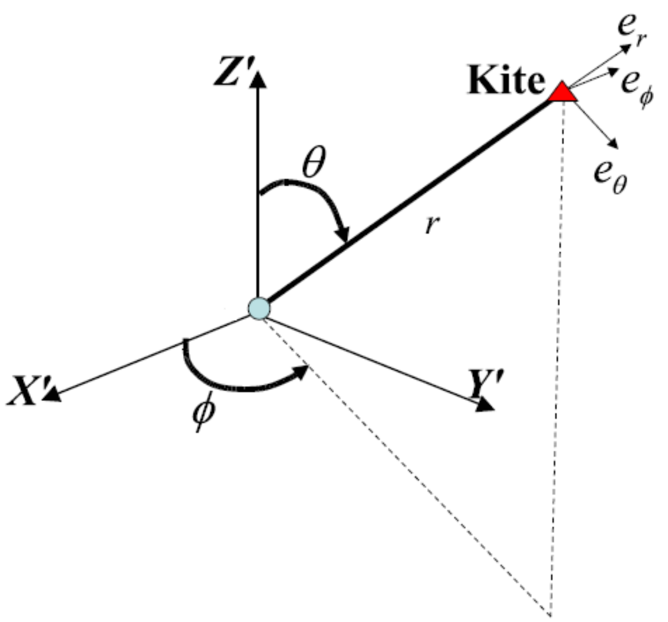


Figure 3.1: Kite model diagram [8].

A fixed Cartesian coordinate system $(X,Y,Z)$ is used (Figure 3.1), with $X$ axis aligned with nominal wind speed vector direction. $\vec{W}_l = \vec{W}_0 + \vec{W}_t$, where $\vec{W}_0$, the nominal wind, is expressed in

$(X,Y,Z)$ as:

$$\vec{W}_0 = \begin{pmatrix} W_x(Z) \\ 0 \\ 0 \end{pmatrix} \tag{3.1}$$

with $W_x(Z)$ being a function that gives the wind speed at an altitude $Z$. The term $\vec{W}_t$ represents the wind turbulence and cannot be predicted exactly. A second Cartesian coordinate system $(X',Y',Z')$ centered at the kite center of gravity is also considered. In this system, the kite position can be expressed as a function of its distance $r$ from the origin and of the angles $\theta$ and $\phi$. Unit vectors $(e_\theta, e_\phi, e_r)$ are expressed in the Cartesian system $(X',Y',Z')$ by:

$$(e_\theta, e_\phi, e_r) = \begin{pmatrix} \cos(\theta)\cos(\phi) & -\sin(\phi) & \sin(\theta)\cos(\phi) \\ \cos(\theta)\sin(\phi) & \cos(\phi) & \sin(\theta)\sin(\phi) \\ -\sin(\theta) & 0 & \cos(\theta) \end{pmatrix} \tag{3.2}$$

Applying Newton's law of motion to the kite in the local coordinate system $(e_\theta, e_\phi, e_r)$, the following dynamic equations are obtained:

$$\begin{aligned} \ddot{\theta} &= \frac{F_\phi}{mr} \\ \ddot{\phi} &= \frac{F_\theta}{mr\sin(\theta)} \\ \ddot{r} &= \frac{F_r}{m} \end{aligned} \tag{3.3}$$

where $m$ is the mass of the kite. The forces $F_\theta$, $F_\phi$, and $F_r$ include the gravity force, $\vec{F}^{grav}$, the apparent force, $\vec{F}^{app}$, the kite aerodynamic force, $\vec{F}^{aer}$ and the traction force, $\vec{F}^{c,trc}$. Their relations, in local coordinates $(e_\theta, e_\phi, e_r)$, are the following:

$$\begin{aligned} F_\theta &= F_\theta^{grav} + F_\theta^{app} + F_\theta^{aer} \\ F_\phi &= F_\phi^{grav} + F_\phi^{app} + F_\phi^{aer} \\ F_r &= F_r^{grav} + F_r^{app} + F_r^{aer} - F_r^{c,trc} \end{aligned} \tag{3.4}$$

Each of the following sections show how each force is taken into account.

### 3.1.1 Gravity Forces

The magnitude of the overall force applied to the kite center of gravity is the sum of the kite weight and the two lines

$$|\vec{F}^{grav}| = \left(m + \frac{\rho_l \pi d_l^2 r}{4}\right) g \tag{3.5}$$

where $g$ is the gravity acceleration, $rho_l$ is the line density and $d_l$ is the diameter of each line. Using the rotation matrix (3.2), the following equations were obtained for the components of $\vec{F}^{grav}$ in the local coordinates $(e_\theta, e_\phi, e_r)$:

$$\vec{F}^{grav} = \begin{pmatrix} F_\theta^{grav} \\ F_\phi^{grav} \\ F_r^{grav} \end{pmatrix} = \begin{pmatrix} \left(m + \frac{\rho_l \pi d_l^2 r}{4}\right) g\sin(\theta) \\ 0 \\ -\left(m + \frac{\rho_l \pi d_l^2 r}{4}\right) g\cos(\theta) \end{pmatrix} \tag{3.6}$$

### 3.1.2 Apparent Forces

The following vector, $\vec{F}^{app}$, accounts for the centrifugal inertial forces:

$$\begin{aligned} F_\theta^{app} &= m(\dot{\phi}^2 r\sin(\theta)\cos(\theta) - 2\dot{r}\dot{\theta}) \\ F_\phi^{app} &= m(-2\dot{r}\dot{\phi}\sin(\theta) - 2\dot{\phi}\dot{\theta} r\cos(\theta)) \\ F_r^{app} &= m(r\dot{\theta}^2 + r\dot{\phi}^2 sin^2(\theta)) \end{aligned} \tag{3.7}$$

### 3.1.3 Kite Aerodynamic Forces

The aerodynamic force, $\vec{F}^{aer}$, depends on the effective wind speed, $\vec{W}_e$. In the local system:

$$\vec{W}_e = \vec{W}_a - \vec{W}_l \tag{3.8}$$

where $\vec{W}_a$ is the kite speed with the ground as reference. It can be expressed in local coordinates as:

$$\vec{W}_a = \begin{pmatrix} \dot{\theta} r \\ \dot{\phi} r\sin(\theta) \\ \dot{r} \end{pmatrix} \tag{3.9}$$

Considering the wind coordinate system with the origin in the kite center of gravity (Figure 3.2). $\vec{x}_w$ is the vector aligned with the effective wind speed vector. $\vec{z}_w$ is the vector contained by the kite longitudinal mirror symmetry plane and pointing from the top surface of the kite to the bottom and $\vec{y}_w$ is the vector completing the right hand system.

The vector $\vec{x}_w$ can be expressed in the local coordinate system $(e_\theta, e_\phi, e_r)$ as:

$$\vec{x}_w = -\frac{\vec{W}_e}{|\vec{W}_e|} \tag{3.10}$$

Using the same coordinate system, $\vec{y}_w$ can be expressed as:

$$\vec{y}_w = e_w(-\cos(\psi)\sin(\eta)) + (e_r \times e_w)(\cos(\psi)\cos(\eta)) + e_r\sin(\psi) \tag{3.11}$$

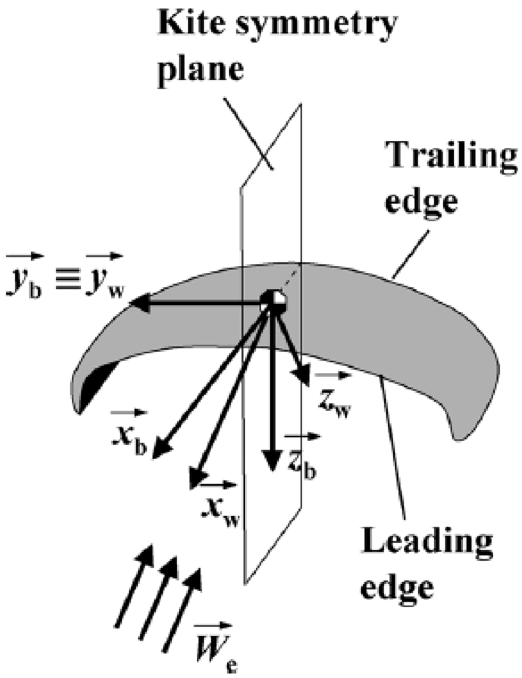


Figure 3.2: Kite wind coordinate system [9].

where:

$$e_w = \frac{\vec{W}_e - e_r(e_r \cdot \vec{W}_e)}{|\vec{W}_e - e_r(e_r \cdot \vec{W}_e)|} \tag{3.12}$$

and

$$\eta = \arcsin\left(\frac{\vec{W}_e \cdot e_r}{\vec{W}_e - e_r(e_r \cdot \vec{W}_e)} \tan(\psi)\right) \tag{3.13}$$

The angle $\psi$ is the control variable and is defined by:

$$\psi = \arcsin\left(\frac{\triangle l}{d}\right) \tag{3.14}$$

where $d$ is the distance between the two lines fixing points at the kite and, $\triangle l$, the length difference of the two lines(Figure 3.3). Angle $\psi$ influences the kite movement by changing the direction of the vector $\vec{F}^{aer}$. Th last vector, $\vec{z}_w$ is defined as:

$$\vec{z}_w = \vec{x}_w \times \vec{y}_w \tag{3.15}$$

Finally, $\vec{F}^{aer}$ in the local coordinate system $(e_\theta, e_\phi, e_r)$ is given by:

$$\vec{F}^{aer} = \begin{pmatrix} \vec{F}^{aer}_\theta \\ \vec{F}^{aer}_\phi \\ \vec{F}^{aer}_r \end{pmatrix} = -\frac{1}{2} C_D A \rho |\vec{W}_e|^2 \vec{x}_w - \frac{1}{2} C_L A \rho |\vec{W}_e|^2 \vec{z}_w \tag{3.16}$$

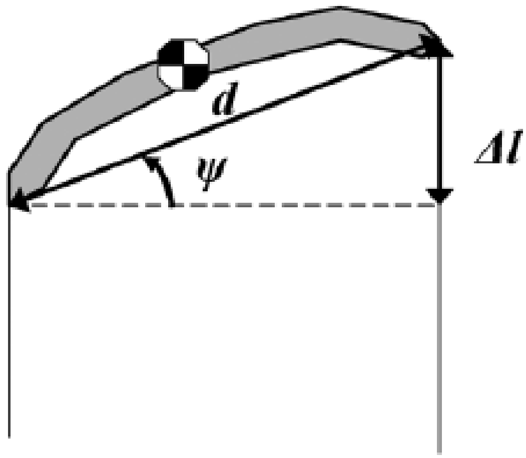


Figure 3.3: Command angle $\psi$ [9].

where $\rho$ is the line density, $A$ is the kite area, $C_L$ and $C_D$ are the kite lift and drag coefficients respectively. $C_L$ is a control input and $C_D = k.C_L^2$, where k is the induced drag constant. The aerodynamic forced induced by the kite lines are not considered during the length of this document, since they have relatively less influence in the kite behaviour than the other forces.

### 3.1.4 Traction Forces

The traction force, $F^{c,trc}$ is directed along the local vector $e_r$ and cannot be negative, since the kite can only pull the lines. This force is measured by a force transducer placed on the ground and trough the use of a controller, it is regulated in such a way that:

$$\dot{r}_{min} \leq \dot{r}(t) \leq \dot{r}_{max} \tag{3.17}$$

where $\dot{r}_{min}$ and $\dot{r}_{max}$ are chosen in order to achieve a good compromise between high line traction force and high line winding speed. Essentially, the stronger the wind, the higher $\dot{r}(t)$ can be, resulting in a higher traction force.

### 3.1.5 Overall Model

The model equations describe the system dynamic in the form:

$$\dot{x}(t) = f(x(t), u(t)W_x(t), \vec{W}_t(t)) \tag{3.18}$$

where $x(t)$ are the model states:

$$x(t) = [\theta(t), \phi(t), r(t), \dot{\theta}(t), \dot{\phi}(t), \dot{r}(t)] \tag{3.19}$$

and $u(t)$ is a control input:

$$u(t) = [\psi(t), C_L, F^{c,trc}] \tag{3.20}$$

More precisely, $\dot{x}(t)$ is written as

$$\begin{bmatrix} \dot{x}_1 \\ \dot{x}_2 \\ \dot{x}_3 \\ \dot{x}_4 \\ \\ \dot{x}_5 \\ \\ \dot{x}_6 \end{bmatrix} = \begin{bmatrix} x_4 \\ x_5 \\ x_6 \\ m({x_5}^2 x_3 \sin(x_1)\cos(x_1) - 2x_6 x_4) + \left(m + \frac{\rho_l \pi d_l^2 x_3}{4}\right) g \sin(x_1) - \\ -\frac{1}{2}k{u_2}^2 A\rho\,(x_4 x_3)^2 (x_5 x_3 \sin(x_1))^2 {x_6}^2 \cos(x_1)\cos(x_5) \\ m(-2x_6 x_5 \sin(x_1) - 2x_5 x_4 r x_3 \cos(x_1)) - \frac{1}{2}k{u_2}^2 A\rho\,(x_4 x_3)^2 (x_5 x_3 \sin(x_1))^2 {x_6}^2 \cos(x_1)\sin(x_5) \\ m(x_3 {x_4}^2 + x_3 {x_5}^2 sin^2(x_1)) - \left(m + \frac{\rho_l \pi d_l^2 x_3}{4}\right) g \cos(x_1) - \\ -\frac{1}{2}k{u_2}^2 A\rho\,(x_4 x_3)^2 (x_5 x_3 \sin(x_1))^2 {x_6}^2 \sin(x_1) - u_3 \end{bmatrix} \tag{3.21}$$

### 3.1.6 Mechanical Power

The mechanical power generated (or spent when the lines are being recovered) by the generator is the algebraic sum of the power generated by recovering and unrolling the kite lines:

$$P(t) = \dot{r}(t) F^{c,trc}(t) \tag{3.22}$$

The mechanical power is then converted to electric power. This process is considered to have an efficiency, $\eta < 1$, to take into account the losses, thus the generated electrical power can be defined by:

$$P_{el}(t) = \eta P(t) \tag{3.23}$$

## 3.2 Wind Model

The increase of wind speed with altitude where stronger and more constant streams usually blow is one of the biggest advantages of this system. Thus, the wind model used during the simulations must depict this situation. The following model will be employed during the simulations carried out in this document:

$$W_x(Z) = W_0 \frac{\ln \frac{Z}{Z_r}}{\ln \frac{Z_0}{Z_r}} \tag{3.24}$$

where $W_0$ is the wind speed at an altitude $Z_0$, $Z$ is the current altitude and $Z_r$ is the roughness factor. Moreover, wind turbulence will be also introduced.

## 3.3 Simulations

In order to verify the model used a simulation was run with the previous model. To solve the ODEs we used the Euler method with a step size, h=0.2. The initial conditions used are presented in table 3.1. In figure 3.4a, we can see the kite trajectory. For the first iterations the kite flies a within the expected limits, but, as expected, without a proper control the kite crashes as can be seen in figure 3.4b.

| | | |
|---|---|---|
| $m$ | 200 | Kite mass $(Kg)$ |
| $A$ | 100 | Kite area $(m^2)$ |
| $g$ | 9.81 | Gravitational constant $(m^2)$ |
| $\rho$ | 1.2 | Air density $(Kg/m^3)$ |
| $W_0$ | 10 | Wind speed $(m/s)$ |
| $\theta_0$ | $\frac{\pi}{2}$ | Radians |
| $\phi_0$ | $\frac{\pi}{4}$ | Radians |
| $r_0$ | 100 | Meters |
| $\dot{\theta}_0$ | 0 | Radians |
| $\dot{\phi}_0$ | $\frac{\pi}{8}$ | Radians |
| $\dot{r}_0$ | 2 | $m/s$ |

Table 3.1: Model and control parameters

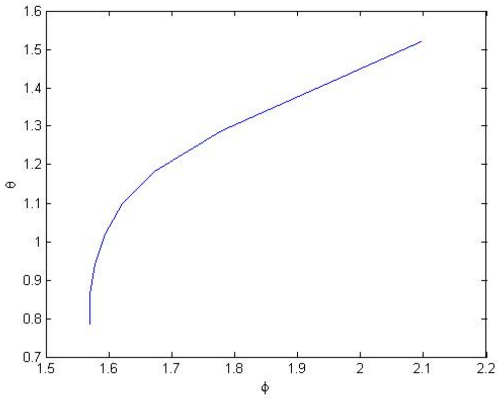


(a) Kite trajectory within limits.

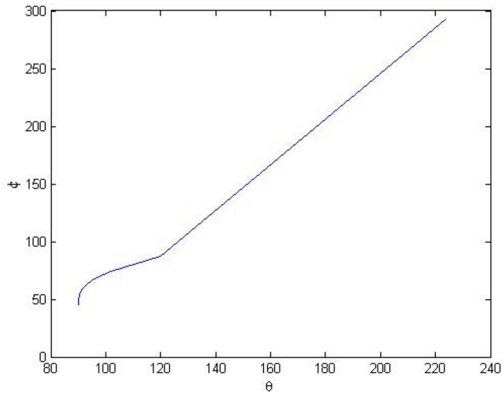


(b) Kite in a collision path.

# Chapter 4

# Control Problem

In this chapter the control problem will be described [8]. The optimal control problem is formulated and a brief introduction to the ACADO tollkit is made [27]. The results obtained are then presented and discussed. Afterwards an introduction to Model Predictive Control (MPC) is made [10] and an approach to the control problem using MPC is used and the respective results presented and discussed.

## 4.1 Control Problem

The control problem objective is to maximize the energy spent during the kite cycle. The cost function used is based in equation (3.22) and is the following:

$$J(t_k) = -\int_{t_k}^{t_k+T_p} \dot{r}(\tau) F^{c,trc}(\tau) d\tau \tag{4.1}$$

To ensure that the kite flies closed loops constraints are used and can be checked in Table 4.2. The kite parameters, constraints and initial values used are presented in the next tables.

| | | |
|---|---|---|
| $m$ | 850 | Kite mass ($Kg$) |
| $A$ | 500 | Kite area ($m^2$) |
| $g$ | 9.81 | Gravitational constant ($m^2$) |
| $\rho$ | 1.2 | Air density ($Kg/m^3$) |
| $W_0$ | 10 | Wind speed ($m/s$) |
| $Z_0$ | 100 | Altitude (m) |
| $Z_r$ | 0.1 | Roughness factor |
| $k$ | 0.04 | Drag constant |

Table 4.1: Model and control parameters

| | |
|---|---|
| $\theta_{min}$ | 35° |
| $\theta_{max}$ | 75° |
| $\|\phi\|_{max}$ | 45° |
| $\dot{r}_{min}$ | -10 |
| $\dot{r}_{max}$ | 10 |
| $\psi_{max}$ | 15° |
| $C_{L,min}$ | 0.1 |
| $C_{L,max}$ | 1.5 |

Table 4.2: Constraints.

### 4.1.1 ACADO toolkit

The ACADO toolkit is an open-source software which implements algorithms for automatic control and dynamic optimization [27]. It provides user friendly interfaces to setup dynamic optimization and model predictive control problems based on a symbolic C++ syntax. It provides a general framework for using a great variety of algorithms for direct optimal control, including MPC as well as state and parameter estimation. It also provides Runge-Kutta and backward differentiation formula (BFD) integrators for the simulation of ordinary differential equations (ODE's) and differential algebraic equations (DAE's). ACADO Toolkit is designed to meet these four key properties:

- Open-source
- User-friendly. The syntax of ACADO Toolkit has been designed to be as intuitive as possible in order to allow the user to formulate control problems in a way that is very close to the usual mathematical syntax.
- Extensible code. It should be easy to link existing algorithms to the toolkit.
- Self-contained. The ACADO Toolkit is written in a completely self-contained manner. No external packages are required, although they can be linked.

The ACADO Toolkit can deal with the following four problem classes:

- Optimal control problems are off-line dynamic optimization problems. These problems aim at calculating open-loop control inputs that minimize a given objective functional while respecting given constraints.
- Multi-objective optimisation and optimal control problems, which require the simultaneous minimisation of more than one objective.
- Parameter and state estimation problems, where parameters, unknown control inputs or initial states are to be identified by measuring an output of a given dynamic system.

- Model predictive control problems and online state estimation, where parametrised dynamic optimisation problems have to be solved repeatedly to obtain a dynamic feedback control law.

### 4.1.2 Implementation using ACADO toolkit

To solve the corresponding problem numerically, the ACADO Toolkit is used. The implementation is based in an ACADO example and adapted to the model presented in the previous chapter. It is important to mention that many locally optimal solutions for this problem exist. In this thesis, we focus on a form of "eight" optimal loop. This route has the advantage of preventing line entanglement. In order to achieve this route, we use the initialization from a text file. With this ACADO tool it is possible to initialize the differential states, controls and parameters . After, the bounds on the variables are used to improve the initial guess. In this case the initialization files are provided in the ACADO toolkit and are based in the results of a previous achieved solution [27]. This ensures that the kite follows a figure of "eight" trajectory and at the same time tries to improve the previously achieved optimal solution using the new constraints.

First of all, the variables are introduced (Figure 4.1a). Then, the parameters (Figure 4.1b).

```
Diferential States:

DifferentialState       r;
DifferentialState     phi;
DifferentialState   theta;

DifferentialState      dr;
DifferentialState    dphi;
DifferentialState  dtheta;

          (...)

Control:

Control               Psi;
```

(a) Variables.

```
PARAMETERS :
double          g =    9.81;
double        rho =    1.23;
double         mk = 2000.00;
double          A =  500.00;
double          V =  720.00;
```

(b) Parameters

Figure 4.1: Extract of the ACADO code

The kite model and the wind model presented in chapter 3 are also introduced (Figure 4.2).

```
Wind Model :

Z        =  r*cos(theta)
w        =  log(Z/Zr) / log(Z0/Zr) *w0
```

Figure 4.2: Wind model code.

The way constraints are implemented in ACADO can be seen in (Figure 4.3)

```
ocp.subjectTo( -0.104   <= Psi   <= 0.104   );
```

Figure 4.3: Example of a constraint in ACADO.

To solve this problem ACADO uses Runge Kutta integrator with order 4/5. The Karush–Kuhn–Tucker (KKT) tolerance, which is used for the convergence criterion of the Sequential quadratic programming (SQP) algorithm has been set to $1e-2$.

The results obtained are given in the next section.

### 4.1.3 Results

The optimal loop is shown in figure 4.4. As expected, it approximates a figure of "eight". In figure 4.5, the line length can be seen. In figure 4.6, the power generated is plotted. As it can be observed, we have to spend around $15MJ$ during the reel in phase to collect the line.

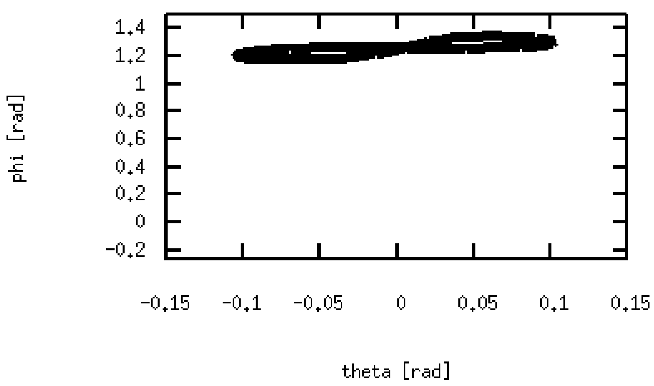


Figure 4.4: Kite orbit.

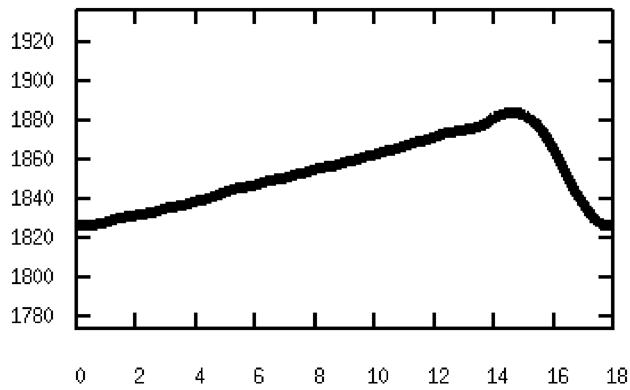


Figure 4.5: Line length.

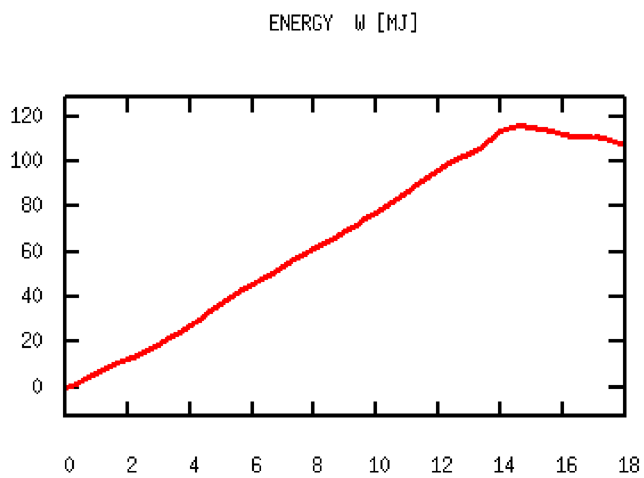


Figure 4.6: Energy at the generator.

## 4.2 Model Predictive Control

The basic MPC concept can be summarized as follows. Suppose there is a need to control a multiple input and output process while satisfying inequality constraints, either in the input and in the output variables. Using a an accurate dynamic model of the process and the current measurements, we can predict future values of the outputs. Then, the appropriate changes in the input variables can be calculated based on both the predictions and measurements. MPC offers several important advantages:

- The process model captures the dynamic and static interactions between input, output, and disturbance variables.
- Constraints on inputs and outputs are considered in a systematic manner.

- The control calculations can be coordinated with the calculation of optimum set points.

- Accurate model predictions can provide early warnings of potential problems.

A block diagram of a model predictive control system is shown in figure 4.7. A process model is used to predict the current values of the output variables. The differences between the actual and the predicted output serve as a feedback signal to the prediction block. The predicted outputs are used in two types of MPC calculations which are performed at each sampling instant: control calculations and set point calculations. Inequality constraints can be included in both calculations.

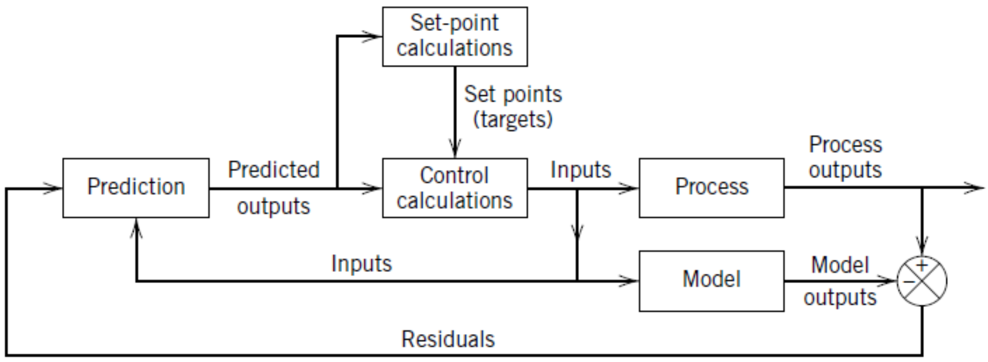


Figure 4.7: Block diagram for model predictive control [10].

The set points for the control calculations are calculated from an economic optimization based on a steady-state model of the process. Typical optimization objectives include maximizing a profit function, minimizing a cost function, etc. The MPC calculations are based on current measurements and predictions of the future values of the outputs. The objective of the MPC control calculations is to determine a sequence of control moves so that the predicted response moves to the set point in an optimal manner. Figure 4.8 shows the actual output $y$, the predicted output $\hat{y}$ and the manipulated input $u$. At the current sampling time, $k$, the MPC strategy calculates a set of $M$ values of the input $\{u(k+i-1), i = 1,2,...,M\}$. The set consists of the current input $u(k)$ and $M-1$ future inputs. The input is held constant after the $M$(control horizon) control moves. The inputs are calculated so that a set of $P$(prediction horizon) predicted outputs $\{\hat{y}(k+i), i = 1,2,...,P\}$ reaches the set point in an optimal manner. The control calculations are obtained in order to optimize an objective function.

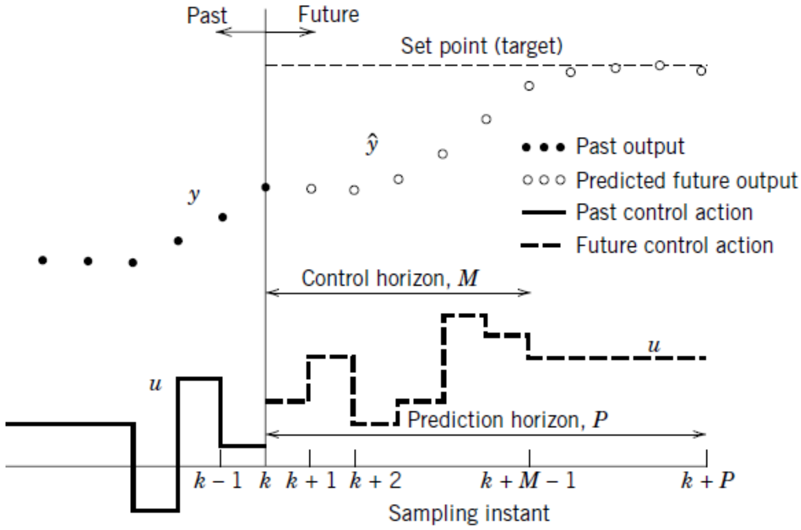


Figure 4.8: MPC example [10].

### 4.2.1 Implementation with ACADO toolkit

In the MPC implentation the objective function (4.1) is used again as well as the restrictions introduced in Table (4.2). The MPC controller is set up using a prediction horizon length of $10s$ and a sampling time of $1s$. To solve the problem ACADO toolkit uses a direct multiple shooting method and a Gauss-Newton Algorithm. The integrator tolerance is defined as $10^{-6}$ and the KKT tolerance as $10^{-5}$. For the prediction model we use the same model introduced before in Chapter 3. The process model is used to simulate wind disturbance. The values of the wind disturbance are read from a file where we can introduce the times and values of the wind disturbance. Then these values are simulated by an ACADO tool called Simulation Environment. This tool simulates computational delays, which means it can delay the control input to the process by the amount of time the controller takes to determine the control inputs. This feature is crucial to study simulations of fast processes where the sampling time is not negligible compared to the settling time of the controlled process.

### 4.2.2 Results

Using the configuration previously reported the following results were obtained. In Figure 4.9 the kite follows the path with no major error. The period of $\phi$ is the double of $\theta$ to prevent line entanglement. In Figure 4.10 a wind turbulence of 10 added to $W_0$ was introduced. As we can see, the control reacts well to this anomaly. The steering device pulls the kite line back during a fraction of time. This can be explained by the small negative peak of speed caused by the controller trying to correct the variation. In Figure 4.11 a wind turbulence of -10 added to $W_0$ was introduced. As we can see, the control also overcomes this anomaly even though $\phi$ takes approximately a full cycle to overcome this issue. This may cause the lines to cross and the kite to fall. In Figure 4.12 a wind turbulence of 15 added to $W_0$ was introduced in two consecutive seconds. As we can see, the kite cannot correct its path. This can cause a crash of the kite or an accident with other near kite since $\phi$ and $\theta$ raise very fast. A similar response is caused when a wind turbulence of -10 added to $W_0$ is introduced.

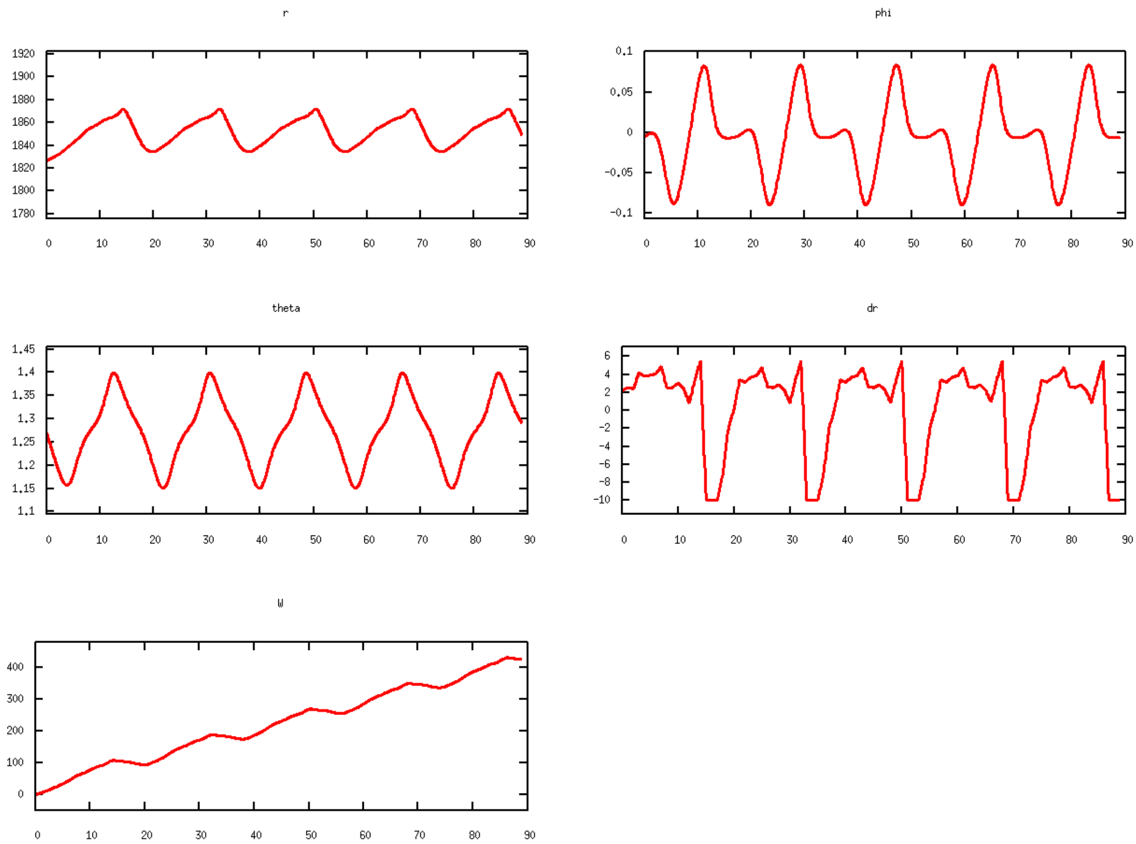


Figure 4.9: Results without wind turbulence.

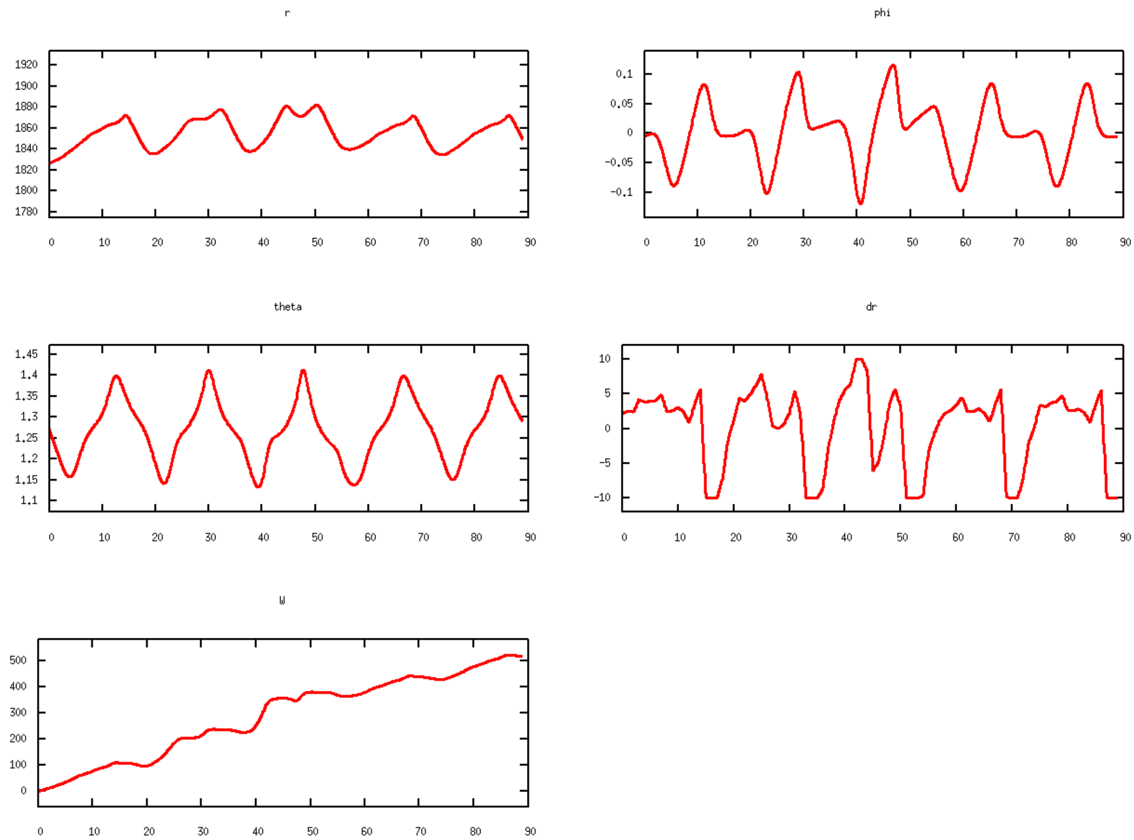


Figure 4.10: Wind turbulence at the instant $t = 50s$.

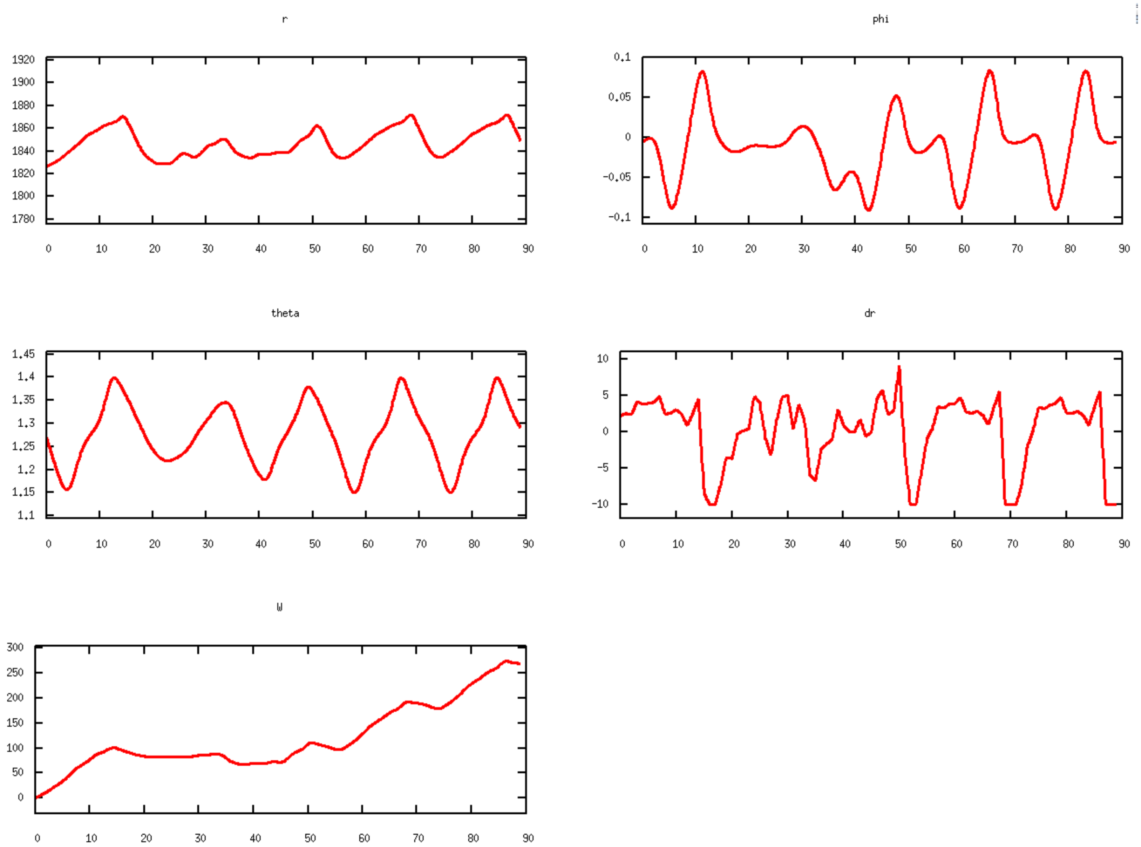


Figure 4.11: Wind turbulence at the instant $t = 20s$.

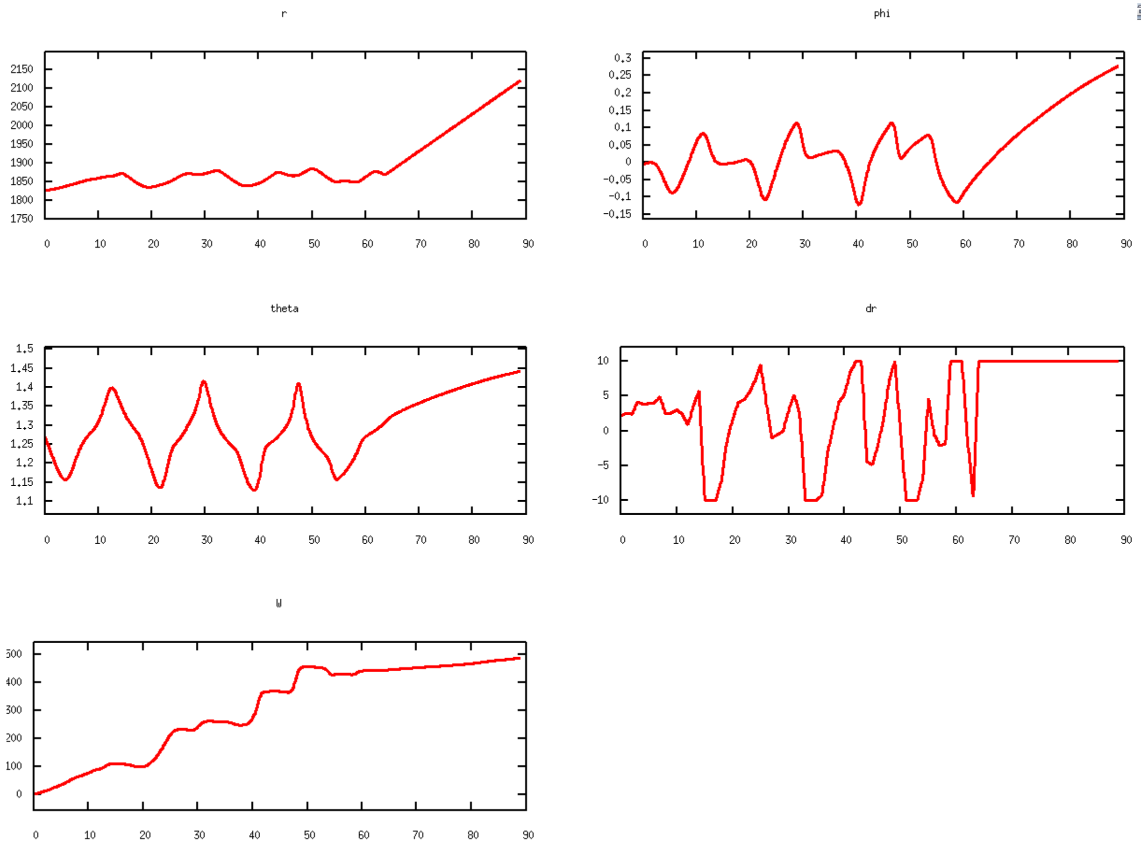


Figure 4.12: Wind turbulence at the instants $t = 50s$ and $t = 51s$.

# Chapter 5

# Conclusion

## 5.1 Summary

This master's dissertation arises in the context of power extraction from high altitude wind. The goal is to study a possible optimal trajectory to improve the efficiency of a laddermill.

As it could be seen in Figure 2.1 Portugal is in the latitude zone where the strongest jet streams are present. This means that this field of research, which looks very promising, could be a good investment for the energy sector.

After reviewing the state of the art of high wind energy systems we concluded that this is actually an emerging research topic with plenty of open problems.

With the work developed during this MSc Dissertation it was possible to get in touch with the topic and the related research problems and challenges. As it could be seen, MPC show very convicing results. It is very robust and can address strong variations of the wind speed. This means, this might be a technology worth investing on.

## 5.2 Further Research

The next immediate step of this project would be to implement the control signals to control the kite actuators and afterwards, to implement the actuators in a real prototype.

# References


[1] Bas Lansdorp and Paul Williams. The laddermill-innovative wind energy from high altitudes in holland and australia. In *Wind Power*, 2006.

[2] Mathias Clinckemaillie. An experimental set-up for energy generation using balanced kites. Master's thesis, KU Leuven, 2012.

[3] BW Roberts and DH Shepard. Unmanned rotorcraft to generate electricity using upper atmospheric winds. In *Australian International Aerospace Congress*, 2003.

[4] Wubbo J Ockels. Laddermill, a novel concept to exploit the energy in the airspace. *Aircraft design*, 4(2):81–97, 2001.

[5] I Argatov, P Rautakorpi, and R Silvennoinen. Estimation of the mechanical energy output of the kite wind generator. *Renewable Energy*, 34(6):1525–1532, 2009.

[6] Cross Product. C. 4 miscellaneous. *Automatic Flight Control of Tethered Kites for Power Generation*, 2012.

[7] Bas Lansdorp, B Remes, and WJ Ockels. Design and testing of a remotely controlled surfkite for the laddermill. In *World Wind Energy Conference, Melbourne, Australia*, 2005.

[8] Massimo Canale, Lorenzo Fagiano, and Mario Milanese. High altitude wind energy generation using controlled power kites. *Control Systems Technology, IEEE Transactions on*, 18(2):279–293, 2010.

[9] Lorenzo Fagiano, Mario Milanese, and Dario Piga. High-altitude wind power generation. *Energy Conversion, IEEE Transactions on*, 25(1):168–180, 2010.

[10] Dale Seborg, Thomas F Edgar, and Duncan Mellichamp. *Process dynamics & control*. John Wiley & Sons, 2011.

[11] Alexander Bolonkin. Using of high altitude wind energy. *Smart Grid and Renewable Energy*, 2(2):75–85, 2011.

[12] Massimo Canale, Lorenzo Fagiano, and Mario Milanese. Kitegen: A revolution in wind energy generation. *Energy*, 34(3):355–361, 2009.

[13] Paul Williams, Bas Lansdorp, and Wubbo Ockesl. Optimal crosswind towing and power generation with tethered kites. *Journal of guidance, control, and dynamics*, 31(1):81–93, 2008.

[14] Boris Houska and Moritz Diehl. Optimal control of towing kites. In *Decision and Control, 2006 45th IEEE Conference on*, pages 2693–2697. IEEE, 2006.

[15] MS Manalis. Airborne windmills and communication aerostats. *Journal of Aircraft*, 13(7):543–544, 1976.

[16] G Riegler, W Riedler, and E Horvath. Transformation of wind energy by a high-altitude power plant. *Journal of Energy*, 7(1):92–94, 1983.

[17] CAJ Fletcher. On the rotary wing concept for jet stream electricity generation. *Journal of Energy*, 7(1):90–92, 1983.

[18] Charles Max Fry and Henry W Hise. Wind driven, high altitude power apparatus, April 11 1978. US Patent 4,084,102.

[19] Alberto Kling. Wind driven power plant, February 14 1978. US Patent 4,073,516.

[20] Paul F Pugh. Wind generator kite system, December 4 1984. US Patent 4,486,669.

[21] William K Watson. Airship-floated wind turbine, January 1 1985. US Patent 4,491,739.

[22] David H Shepard. Power generation from high altitude winds, April 21 1987. US Patent 4,659,940.

[23] Bas Lansdorp and WJ Ockels. Comparison of concepts for high-altitude wind energy generation with ground based generator. In *Proceedings of the NRE 2005 Conference, Beijing, China*, pages 409–417, 2005.

[24] Uwe Fechner and Roland Schmehl. Design of a distributed kite power control system. In *Control Applications (CCA), 2012 IEEE International Conference on*, pages 800–805. IEEE, 2012.

[25] L Fagiano, AU Zgraggen, M Khammash, and M Morari. On control of tethered wings for airborne wind energy. In *American Control Conference (ACC), 2013*, pages 1430–1435. IEEE, 2013.

[26] Moritz Diehl. Real-time optimization for large scale nonlinear processes. 2001.

[27] Boris Houska, Hans Joachim Ferreau, and Moritz Diehl. Acado toolkit—an open-source framework for automatic control and dynamic optimization. *Optimal Control Applications and Methods*, 32(3):298–312, 2011.

[28] Timm Faulwasser and Rolf Findeisen. Nonlinear model predictive path-following control. In *Nonlinear Model Predictive Control*, pages 335–343. Springer, 2009.

[29] Fernando ACC Fontes. A general framework to design stabilizing nonlinear model predictive controllers. *Systems & Control Letters*, 42(2):127–143, 2001.

[30] Fernando ACC Fontes, Dalila BMM Fontes, and Amélia CD Caldeira. Model predictive control of vehicle formations. In *Optimization and Cooperative Control Strategies*, pages 371–384. 2009.